RSC Advances

PAPER

View Article Online
View Journal | View Issue

Cite this: *RSC Adv.*, 2022, **12**, 4469

Catalytic decomposition of hydroxylamine nitrate and hydrazine nitrate using Ru/ZSM-5 catalyst under mild reaction conditions†

Zhipeng Zhang, ‡ Baole Li, ‡ Qi Chen, Xiwen Chen, Taihong Yan, Weifang Zheng* and Chen Zuo*

Received 19th October 2021
Accepted 20th December 2021

DOI: 10.1039/d1ra07724d

rsc.li/rsc-advances

Hydroxylamine nitrate and hydrazine nitrate are dangerous explosives and toxic chemicals. Catalytic decomposition is an efficient way for disposal of these chemicals. In the current work, a Ru/ZSM-5 catalyst has been fabricated and evaluated for the decomposition of hydroxylamine nitrate and hydrazine nitrate in 1.0 mol L^{-1} HNO_3. The hydroxylamine nitrate and hydrazine nitrate can be thoroughly decomposed under 80 °C. And the Ru/ZSM-5 catalyst can be separated from the reaction mixture and reused at least 130 times with stable catalytic performance. Easy operation, less solid waste generation, and a simple catalytic device make the strategy reported here practical, environmentally friendly, and economically attractive.

1. Introduction

In the Purex process, Pu(IV) is reduced by the reducing reagent hydroxylamine nitrate (HAN), and hydrazine nitrate (HN) acts as a stabilizer.[1,2] In the reducing process, a waste liquid containing nitric acid (0.8–1.8 mol L^{-1}), hydroxylamine nitrate (0.3 mol L^{-1}) and hydrazine nitrate (0.1 mol L^{-1}) is generated.[3] To reduce the amount of secondary radioactive waste, a large amount of raffinates containing nitric acid and reducing agents used should be handled through the process of continuous evaporation and denitration.[4] However, the presence of hydroxylamine nitrate and hydrazine nitrate in aqueous waste is undesirable, because it often makes the treatment of liquid radioactive waste complex. Furthermore, hydrazine, which is capable of reacting with nitrous acid to form explosive hydrazoic acid, is a potentially hazardous chemical compound in the course of chemical denitration, and hydroxylamine nitrate has been involved in several incidents due to its instability and autocatalytic nature.[5] Therefore, it is necessary to decompose hydroxylamine nitrate and hydrazine nitrate to provide the final safe disposal of radioactive waste liquid. The most common methods for the decomposition of hydroxylamine nitrate and hydrazine nitrate in HNO_3 are adding excess $NaNO_2$ (reaction (1)) or passing in N_2O_4 gas (reaction (2)). However, adding excess $NaNO_2$ will generate large amounts of radioactive solid waste (approximately 17 kg of sodium salt are produced for disposing of one ton of waste liquid). And the method passing excess N_2O_4 gas into waste liquid suffers from several drawbacks, such as large amounts of radioactive gas being generated and complicated operation. Therefore, the development of easy operation, inexpensive and environmentally friendly methods of decomposing hydrazine is still a challenging research topic.

A lot of research has been reported on the catalytic decomposition of hydrazine and hydroxylamine as monopropellants.[6–11] Recently, a new high temperature tolerant catalyst based on cobalt doped cerium oxide that was found to be both thermally and chemically stable under monopropellant decomposition conditions was developed by Ruchika and the kinetics and mechanism of the thermal decomposition and catalytic decomposition of hydroxylamine nitrate were studied.[12,13] Heterogeneous catalytic decomposition of hydroxylamine nitrate has not been reported in the HNO_3 system. Among various metal catalysts proposed for hydrazine decomposition, noble metals, such as Ru and Pt, exhibited good catalytic activity and stability in acid solutions.[14,15] However, only several examples have been reported focusing on the kinetics and mechanism of catalytic decomposition of hydrazine,[16–20] which proves that heterogeneous catalysis (reaction (3)) is a promising method for the decomposition of hydrazine and heterogeneous catalytic decomposition of hydroxylamine nitrate has not been reported in HNO_3 system. This method is simple and available, which offers several advantages: (i) reduced solid radioactive waste, (ii) ease of operation, (iii) simple device structure, (iv) small reactor volume. Therefore, the further development of an efficient and stable catalytic system to catalytically decompose hydrazine in the HNO_3 system is a very important subject.

Chinese Institute of Atomic Energy, PO Box 275(126), Beijing 102413, China. E-mail: zchen_2008@126.com

† Electronic supplementary information (ESI) available. See DOI: 10.1039/d1ra07724d

‡ The first two authors contributed equally to this work.

$$N_2H_5NO_3 + NaNO_2 \rightarrow N_2\uparrow + N_2O\uparrow + NaNO_3 + H_2O \quad (1)$$

$$N_2H_5NO_3 + N_2O_4 \rightarrow N_2\uparrow + N_2O\uparrow + HNO_3 + H_2O \quad (2)$$

$$N_2H_5NO_3 \xrightarrow{Ru} NH_4NO_3 + N_2\uparrow + N_2O\uparrow + HNO_3 + H_2O \quad (3)$$

ZSM-5 type acid zeolites[21–25] have been widely used in catalysis because of their excellent features such as strong acidity, superior hydrothermal stability, unique shape selectivity and so on. Based on the above consideration, herein we reported an acid-stable catalyst Ru/ZSM-5, which simultaneously achieved the complete decomposition of hydroxylamine nitrate (0.3 mol L^{-1}) and hydrazine nitrate (0.1 mol L^{-1}) in 1.0 mol L^{-1} HNO_3 under moderate conditions (80 °C). The study of this work may be of great significance for the effective treatment of waste liquid containing hydrazine nitrate and hydroxylamine nitrate in reprocessing plants.

2. Experimental section

2.1 Materials and regents

$RuCl_3 \cdot xH_2O$ (AR, 38% wt Ru), HNO_3 (AR, 68 wt%) and hydrazine hydrate (AR, 55 wt%) were purchased from Macklin Reagent Co., Ltd (Shanghai, China). Hydrazine nitrate was prepared by the neutralization reaction of hydrazine hydrate and nitric acid. Hydroxylamine nitrate was produced from hydroxylamine hydrochloride by ion exchange method with strong acid cation resin. Commercially available ZSM-5 sphere (Si/Al = 365) was purchased from Xianfeng Nano Co., Ltd and dried at 100 °C for 12 h before use. Ru/TiO_2 and Ru/SiO_2 catalysts were purchased from Kaili Catalyst & New Materials Co., Ltd (Xian, China).

2.2 Preparation of Ru supported zeolite catalyst Ru/ZSM-5

The synthesis of the Ru/ZSM-5 catalysts can be illustrated as shown in Scheme 1. The synthesis can be divided into two main steps: (i) the impregnation of Ru on the ZSM-5 support by wet-impregnation method; (ii) calcination and reduction of the Ru/ZSM-5 catalysts.

The Ru supported zeolites was prepared by a wet impregnation method. Typically, $RuCl_3 \cdot xH_2O$ (1.84 g 38% wt Ru precursor) was dissolved in 10 mL of deionized water, and it was then added into 10 g of zeolite (particle size, manufacturer) under stirring at room temperature for 24 h. The solvent was then removed by vacuum-rotating evaporator, and the sample was dried in an oven at 100 °C for 12 h. Finally, the impregnated catalyst was calcined and reduced by 5% hydrogen and nitrogen mixture at 450 °C for 5 h to obtain the Ru/ZSM-5 catalyst.

2.3 Characterization of catalysts

X-ray diffraction (XRD) patterns were recorded with a Rigaku D/max-2400 diffractometer, using Cu Kα (λ = 0.15432 nm) operated, in the 2θ range from 3° to 90°. The specific surface areas of the prepared materials were measured by nitrogen adsorption–desorption isotherms at 77 K after degassing the samples using a Micromeritics Model ASAP 2010 instrument. The specific surface area of the sample was measured by the BET method.

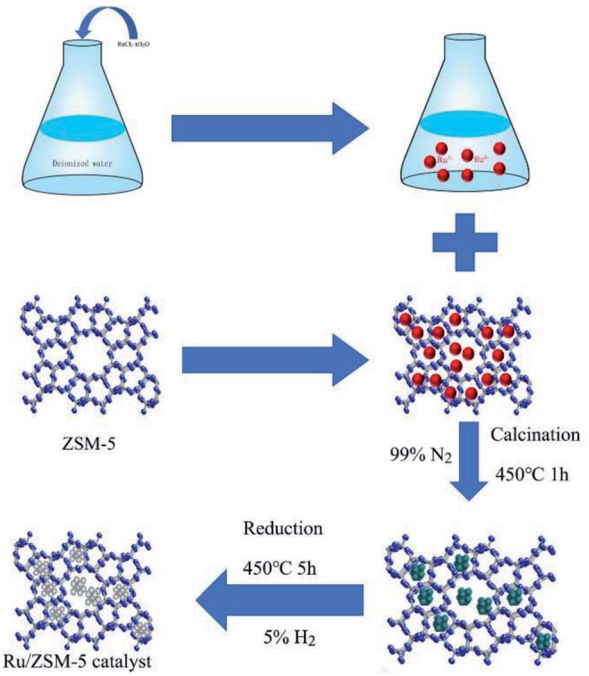

Scheme 1 Synthesis of Ru/ZSM-5 catalyst.

The structure of Ru/ZSM catalysts was observed by transmission electron microscopy (TEM, Tecnai G2 F30). X-ray photoelectron spectroscopy (XPS, PHI-5702) was recorded to investigate the chemical state and elemental composition of the catalyst. Elemental analysis and inductively coupled plasma atomic emission spectroscopy (ICP-AES) were employed to measure the actual content of Ru in the material. Simultaneously, the content of Ru after reaction was also analyzed to determine the amounts of these species leached into the solution.

2.4 Catalytic testing

The decomposition reaction of hydroxylamine nitrate and hydrazine nitrate in HNO_3 was operated using a batch reactor system. In a typical procedure, 2 g of unreduced catalyst, 20 mL of liquid (0.3 mol L^{-1} HAN and 0.1 mol L^{-1} HN in 1.0 mol L^{-1} HNO_3) to be treated, were loaded in a round-bottom flask equipped with a reflux condenser and exhaust gas absorption device at 80 °C. After the reaction was completed, the catalyst was separated from the reaction mixture by simple filtration and then reused directly in model reaction for the next round without further purification.

3. Results and discussion

3.1 Catalyst characterization

The Ru/ZSM-5 catalysts were fully characterized by N_2 adsorption at 77 K using Brunauer–Emmett–Teller (BET), powder X-ray diffraction (XRD), transmission electron microscopy (TEM) and SEM energy dispersive X-ray spectroscopy (EDS), and X-ray photoelectron spectroscopy (XPS).

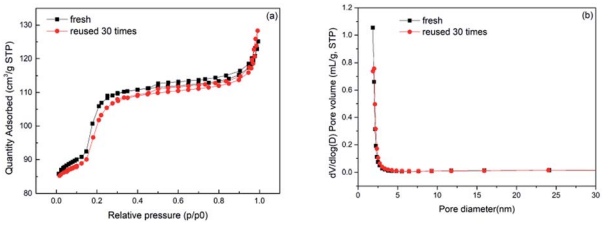

Fig. 1 N_2 adsorption and desorption isotherms (a) and corresponding pore size distributions (b) of fresh and used Ru/ZSM-5 catalysts.

Table 1 Physical and chemical properties of the fresh and reused Ru/ZSM-5 catalysts

Catalysts	S_{BET} ($m^2\ g^{-1}$)	Pore volume ($cm^3\ g^{-1}$)	Pore size (nm)
Ru/ZSM-5 (fresh)	359.86	0.193449	1.5008
Ru/ZSM-5 (used)	346.99	0.198479	1.5413

The Ru metal amount of the immobilized catalyst was found to be 4.95% wt Ru based on inductively coupled plasma atomic emission spectroscopy (ICP-AES) analysis. The textural properties of the fresh and 30 times reused catalysts were analyzed by N_2 adsorption–desorption isotherms. As shown in Fig. 1a, the isotherms of the fresh and used catalysts exhibited a combination of type I and type IV isotherms,[26] indicating that the Ru/ZSM-5 catalyst was typical of mesoporous structured material containing also a certain of amounts of micropores, which was consistent with corresponding BJH pore size distribution denoted in Fig. 1b. The pore size distribution, BET surface areas and pore volumes of the fresh and used catalysts were shown in Table 1. The surface areas of the Ru/ZSM-5 catalyst slightly decreased after 30 cycles, while the pore volume and pore size distribution remained essentially unchanged. From these results, it is obvious that the prepared Ru/ZSM-5 catalyst is stable enough to endure the hydrothermal nitric acid conditions.

Fig. 2 shows the XRD patterns of ZSM-5(a), Ru/ZSM-5(b) and Ru/ZSM-5 reused 130 times(c) samples respectively. All samples displayed similar unique characteristic peaks of MFI structure at $2\theta = 7$–$10°$, 22–35° and 45°, suggesting that introduction of ruthenium species, and catalytic decomposition reaction process made little change in the topology structure of ZSM-5.[27] Ruthenium species diffraction peaks at $2\theta = 38.6°$ and 44.2° along with an additional weak reflection at 58.4° were observed in the patterns of Ru/ZSM-5(b) and used Ru/ZSM-5(c) samples, which corresponded to the (100), (101) and (102) reflections, respectively.[28,29] It is apparent that these diffraction peaks are consistent with the diffraction planes of bulk hexagonal ruthenium metal (JCPDS-ICDD card No. 06-0663).[30]

The SEM images of fresh and 130 times reused Ru/ZSM-5 are shown in Fig. S1.† The SEM micrographs present that the fresh catalyst particles are stacked in rods, the diameter of a single rod is about 2–10 μm, and the length is about 15–20 μm. It can be seen from the Fig. S1(c and d)† that the shape of the 130 times reused catalyst did not change obviously.

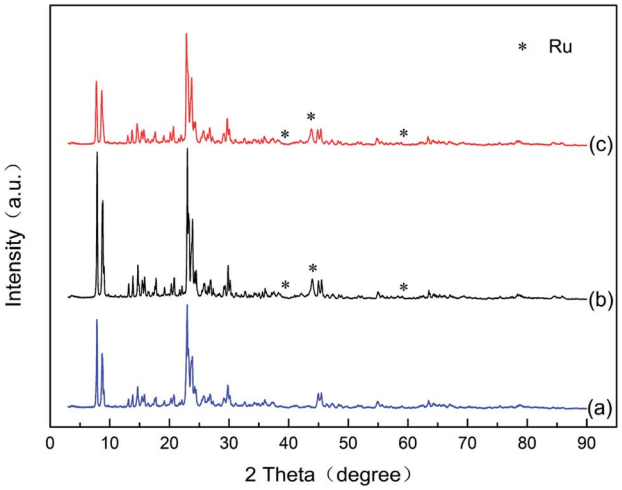

Fig. 2 XRD patterns of ZSM-5 and 5% Ru/ZSM-5 samples (a) ZSM-5, (b) 5% Ru/ZSM-5 (fresh), (c) 5% Ru/ZSM-5 (reused).

The TEM images of Ru/ZSM-5(a) and Ru/ZSM-5 reused 130 times(b) samples are shown in Fig. 3. The average diameter of ruthenium particles was figured out to be about 6.9 nm for the fresh catalyst by Nano Measure software. For used Ru/ZSM-5 samples, the obvious size growth of ruthenium particles was observed as shown in Fig. 3b with ruthenium particles size about 10.5 nm, which led to the reduction of the amount of active sites on the surface of the catalyst. Furthermore, element

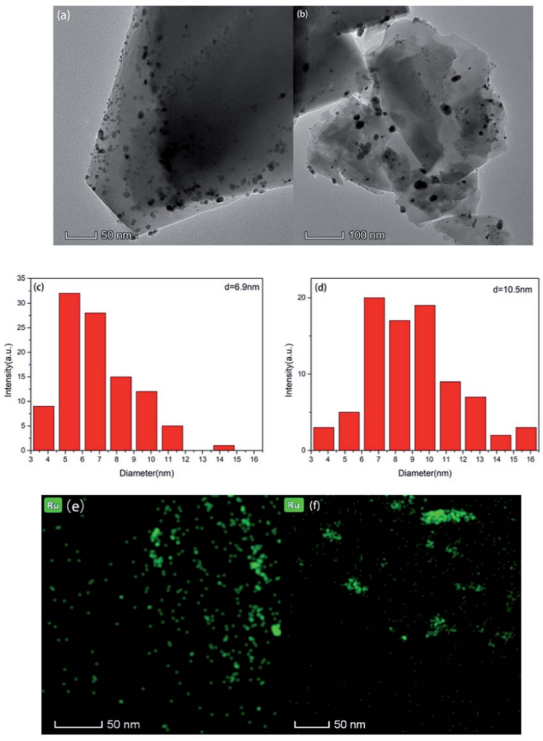

Fig. 3 TEM images and ruthenium particle size distributions as well as ruthenium elemental mapping images of fresh Ru/ZSM-5 catalysts (a, c and e) and used Ru/ZSM-5 catalysts (b, d and f).

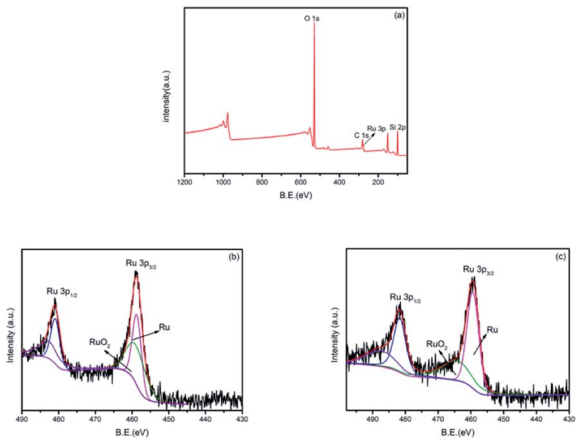

Fig. 4 XPS full spectrum of (a) fresh Ru/ZSM-5 and Ru 3p XPS spectra of Ru/ZSM-5 (b) fresh catalyst, (c) used catalyst.

Table 2 XPS results of fresh and reused Ru/ZSM-5 catalysts

		Peak area		
Catalyst	Ru species	$3p_{3/2}$	$3p_{1/2}$	Ru^0/Ru^{4+}
Fresh	Ru^{4+}	3545.697	1450.118	2.14
	Ru^0	6398.616	4267.877	
Used	Ru^{4+}	6468.229	4314.309	1.49
	Ru^0	9654.702	6439.687	

mapping was adopted in order to further describe the spatial distribution of ruthenium particles. As a result, it confirmed ruthenium particles were well dispersed on the surface of fresh Ru/ZSM-5 samples, and the aggregation of ruthenium nanoparticles and reduction of catalytic active sites in the used Ru/ZSM-5 samples, which was also in a good agreement with the results from TEM. In order to determine the amount of ruthenium located inside the channel, the fresh Ru/ZSM-5 catalyst was further characterized by HR-TEM. As shown in Fig. S2,† the ruthenium content located inside the channels was very low.

XPS was performed to determine the chemical elements present in the Ru/ZSM-5 catalyst and to explain the possible reason of inactivation. Based on the XPS wide scan spectra, Ru/ZSM-5 catalyst was found to contain C, Si, Ru and O elements (Fig. 4a). The ruthenium XPS spectra of sample fresh Ru/ZSM-5 (Fig. 4b) is compared with that of Ru/ZSM-5 reused 130 times (Fig. 4c). It can be seen that two Ru species are discriminated in fresh Ru/ZSM-5 and used Ru/ZSM-5 with binding energies around 462.2 eV and 463.5 eV, which are ascribed to Ru(0) and RuO_2, respectively, confirming that RuO_2 species on the surface of ZSM-5 are converted partially to metallic Ru species during reduction.[31] As shown in Table 2, in fresh Ru/ZSM-5, the majority of surface ruthenium species is contributed to Ru(0), which accounts for about 68%, whereas in used Ru/ZSM-5, the portion of surface Ru(0) species is about 59%. It is possible that Ru(0) species on the catalyst was gradually oxidized and transformed into RuO_2 species as the number of cycles increased.

Table 3 Catalytic performances for the decomposition of hydroxylamine nitrate and hydrazine nitrate[a]

Entry	Catalyst	Time (min)	HAN decomposition rate (%)	HN decomposition rate (%)
1	No	60	1.0	1.88
2	ZSM-5	60	1.1	1.98
3	Ru/ZSM-5	38	100	100
4	Ru/TiO_2	60	71.2	31.5
5	Ru/SiO_2	60	78.5	28.4

[a] Reaction conditions: T = 80 °C, C_{HN} = 0.1 mol L^{-1}, C_{HAN} = 0.3 mol L^{-1}, C_{HNO_3} = 1.0 mol L^{-1}, 2.0 g 5% Ru/ZSM-5.

3.2 Catalytic decomposition reaction conditions

The activity of the prepared catalyst was tested for the reaction of decomposition of hydroxylamine nitrate (0.3 mol L^{-1}) and hydrazine nitrate (0.1 mol L^{-1}) in 1.0 mol L^{-1} HNO_3 at 80 °C. The reaction, as shown in Table 3, proceeded very slowly in the absence of catalyst (Table 3, entry 1) or in the presence of ZSM-5 (Table 3, entry 2), and both hydroxylamine nitrate and hydrazine nitrate had a low decomposition rate after heating for 60 min (Table 3, entry 1). Pleasingly, when Ru/ZSM-5 was used as the catalyst, the decomposition rate of hydroxylamine nitrate and hydrazine nitrate reached 100% (Table 3, entry 3). Ru/TiO_2 (Table 3, entry 3) and Ru/SiO_2 as catalyst (Table 3, entry 4) were examined, but no better result was obtained. Nitrogen oxides and nitrogen were the main products.[32]

The effect of the reaction temperature on the decomposition rate of hydroxylamine nitrate and hydrazine nitrate were examined in 1.0 mol L^{-1} HNO_3, as shown in Table 4. The decomposition rate slowly increased with the raised reaction temperature from 50 °C to 70 °C (Table 4, entries 1–3), but rapidly increased to 100% at 80 °C (Table 4, entry 4). The experiment of catalytic decomposition of nitric acid showed that the concentration of nitrous acid increased obviously by increasing the temperature above 80 °C (Fig. S3†), which increased the decomposition rate of hydrazine nitrate and hydroxylamine nitrate and shorten the reaction time significantly.[33,34] And increasing the reaction temperature to 90 °C made the decomposition reaction violent (Table 4, entry 5). These results indicated that the reaction temperature is a significant factor to regulate the decomposition rate. At the present reaction conditions, the suitable temperature was selected at 80 °C.

Under the condition of 80 °C and 1.0 mol L^{-1} HNO_3, the effect of different amount of catalyst on the decomposition reaction was listed in Table 5. It can be seen that the reaction time significantly reduced from 190 min to 38 min with the elevated amount of catalyst from 0.3 g to 2.0 g. It may be the decrease in the amount of catalysts lead to a reduction in the active sites, so the reaction time was prolonged. Therefore, from the single-factor experiment results, the appropriate reaction conditions is obtained that reaction temperature is 80 °C and the amount of Ru/ZSM-5 catalyst is 2.0 g in the decomposition reaction of hydroxylamine nitrate and hydrazine nitrate.

Table 4 The influence of reaction temperature on the catalytic performance of Ru/ZSM-5 for the decomposition of hydrazine and hydroxylamine[a]

Entry	Catalyst	Temperature (°C)	Time (min)	HAN decomposition rate (%)	HN decomposition rate (%)
1	Ru/ZSM-5	50	60	6.29	12.28
2	Ru/ZSM-5	60	60	5.56	14.08
3	Ru/ZSM-5	70	60	19.24	34.32
4	Ru/ZSM-5	80	38	100	100
5	Ru/ZSM-5	90	24	100	100

[a] Reaction conditions: $T = 50$–90 °C, $C_{HN} = 0.1$ mol L^{-1}, $C_{HAN} = 0.3$ mol L^{-1}, $C_{HNO_3} = 1.0$ mol L^{-1}, 2.0 g 5% Ru/ZSM-5.

Table 5 The influence of the catalyst amounts on the reaction duration for achieving the 100% decomposition of hydrazine and hydroxylamine[a]

Entry	Catalyst	Catalyst quality (g)	Time (min)
1	Ru/ZSM-5	2.0	38
2	Ru/ZSM-5	1.5	60
3	Ru/ZSM-5	1.2	65
4	Ru/ZSM-5	0.9	78
5	Ru/ZSM-5	0.6	130
6	Ru/ZSM-5	0.3	190

[a] Reaction conditions: $T = 80$ °C, $C_{HN} = 0.1$ mol L^{-1}, $C_{HAN} = 0.3$ mol L^{-1}, $C_{HNO_3} = 1.0$ mol L^{-1}, 0.3–2.0 g 5% Ru/ZSM-5.

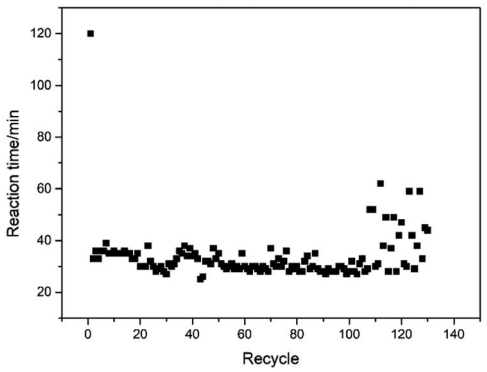

Fig. 5 Stability test of Ru/ZSM-5 catalyst for the decomposition of hydrazine and hydroxylamine.

To investigate the effect of nitric acid concentration on the catalytic decomposition reaction, we performed a series of experiments and the results were shown in the Table 6. An increase in the HNO_3 concentration in the range 0.8–1.8 mol L^{-1} HNO_3 made the reaction time decrease from 48 min to 11 min.

This phenomenon is consistent with the Avaniev's research results under the condition of 1% Pt/SiO_2 catalyst.[34] It may be attributed to the increase in the amount of nitrous acid with the increase of nitric acid concentration (Fig. S4†), which promotes the decomposition of hydroxylamine nitrate and hydrazine nitrate.[35]

3.3 Recyclability of the catalyst

Finally, the catalyst recyclability (Fig. 5) has been tested in the presence of 2.0 g Ru/ZSM-5 catalyst at 80 °C in 1.0 mol L^{-1} HNO_3. In this procedure, the catalyst was separated from the reaction mixture by simple filtration. The recovered catalyst was washed with deionized water, and then reused directly in model reaction for the next round without further purification. It was found that the catalyst could be reused at least 130 times under the same reaction conditions without the requirement to add any additional catalyst. One hundred and thirty runs can be efficiently performed with 100% decomposition rate of hydroxylamine nitrate and hydrazine nitrate.

After the 130th cycle, the reused catalyst was analyzed by XRD (Fig. 2), and the results showed that the catalyst maintained its structural integrity. In order to confirm the morphological stability of the catalyst, TEM (Fig. 3) analysis was also performed, indicating the aggregation of ruthenium nanoparticles and reduction of catalytic active sites in the reused Ru/

Table 6 Comparison of activity for hydroxylamine and hydrazine decomposition tests over different concentration of nitric acid[a]

Entry	Catalyst	C_{HNO_3} (mol L^{-1})	Time (min)	HAN decomposition rate (%)	HN decomposition rate (%)
1	Ru/ZSM-5	0.8	48	100	100
2	Ru/ZSM-5	1.0	38	100	100
3	Ru/ZSM-5	1.2	31	100	100
4	Ru/ZSM-5	1.4	16	100	100
5	Ru/ZSM-5	1.6	12	100	100
6	Ru/ZSM-5	1.8	11	100	100

[a] Reaction conditions: $T = 80$ °C, $C_{HN} = 0.1$ mol L^{-1}, $C_{HAN} = 0.3$ mol L^{-1}, $C_{HNO_3} = 0.8$–1.8 mol L^{-1}, 2.0 g 5% Ru/ZSM-5.

ZSM-5 samples. The leaching amount of Ru was also determined by inductively coupled plasma technology. It was found that the content of Ru was reduced from 4.95% wt to 2.78% wt after the 130th cycle. The ruthenium XPS (Fig. 4) spectra confirmed Ru(0) species on the surface of ZSM-5 decreased over fresh Ru/ZSM-5. These results indicate that the increase in reaction time after the 110th run is due to the growth and loss of Ru particles, and change of Ru valence state, which simultaneously led to the reduction of catalyst activity.

4. Conclusions

In summary, Ru/ZSM-5 was successfully prepared and confirmed using XRD, BET, TEM, ICP-AES, and XPS techniques. The Ru/ZSM-5 catalyst was shown to be an efficient heterogeneous catalyst for decomposition of hydroxylamine nitrate and hydrazine nitrate at 80 °C in 1.0 mol L^{-1} HNO_3. The catalyst could be easily recovered by simple filtration and reused 130 times without significant loss of activity, showing good potential for industrial application. The characterization results showed that the catalyst maintained its MFI structure after long-term reaction and the ruthenium nanoparticles agglomerated and gradually transformed into oxidized state leading to the decrease in catalyst activity. This conclusion may have a guiding role in optimizing the preparation method of the catalyst.

Conflicts of interest

The authors declare that they have no known competing financial interests or personal relationships that could have appeared to influence the work reported in this paper.

References

1 A. V. Anan'ev and V. P. Shilov, *Radiochemistry*, 2006, **48**, 105–118.
2 A. A. Bessonov, A. V. Gogolev, V. P. Shilov, A. V. Anan'ev and A. M. Fedoseev, *Radiochemistry*, 2011, **53**, 244–249.
3 A. V. Ananiev, J. C. Broudic and P. Brossard, *Appl. Catal., A*, 2003, **242**, 1–10.
4 M. Ristić, S. Musić, M. Marciuš, S. Krehula, E. Kuzmann and Z. Homonnay, *J. Radioanal. Nucl. Chem.*, 2019, **322**, 1477–1485.
5 A. V. Ananiev, I. G. Tananaev and V. P. Shilov, *Russ. Chem. Rev.*, 2005, **74**, 1039–1059.
6 S. M. Ciborowski, R. Buszek, G. Liu, M. Blankenhorn, Z. Zhu, M. A. Marshall, R. M. Harris, T. Chiba, E. L. Collins, S. Marquez, J. A. Boatz, S. D. Chambreau, G. L. Vaghjiani and K. H. Bowen, *J. Phys. Chem. A*, 2021, **125**, 5922–5932.
7 S. D. Chambreau, D. M. Popolan-Vaida, G. L. Vaghjiani and S. R. Leone, *J. Phys. Chem. Lett.*, 2017, **8**, 2126–2130.
8 T. Urbanski, *Chemistry and Technology of Explosives*, Pergamon Press, New York, 1967.
9 A. V. Ananiev, J. C. Broudic and P. Brossard, *Appl. Catal., A*, 2003, **242**, 1–10.
10 Y. P. Qiu, L. L. Zhou, Q. Shi and P. Wang, *Chem. Commun.*, 2021, **57**, 623–626.
11 F. Zheng, H. Dong, Y. Ji and Y. Li, *Appl. Surf. Sci.*, 2019, **469**, 316–324.
12 R. Agnihotri and C. Oommen, *RSC Adv.*, 2018, **8**, 22293–22302.
13 R. Agnihotri and C. Oommen, *Propellants, Explos., Pyrotech.*, 2021, **46**, 286–298.
14 C. J. Koh, C. L. Liu, C. W. Harmon, D. Strasser, A. Golan, O. Kostko, S. D. Chambreau, G. L. Vaghjiani and S. R. Leone, *J. Phys. Chem. A*, 2011, **115**, 4630–4635.
15 S. D. Chambreau, C. J. Koh, D. M. Popolan-Vaida, C. J. Gallegos, J. B. Hooper, D. Bedrov, G. L. Vaghjiani and S. R. Leone, *J. Phys. Chem. A*, 2016, **120**, 8011–8023.
16 A. V. Anan'ev, M. Y. Boltoeva, N. L. Sukhov, G. L. Bykov and B. G. Ershov, *Radiochemistry*, 2004, **46**, 578–582.
17 A. V. Anan'ev and V. P. Shilov, *Radiochemistry*, 2006, **48**, 133–135.
18 E. Belova, E. Nazin, A. Smirnov and A. Obedkov, *Prog. Nucl. Energy*, 2021, **141**, 103968.
19 A. V. Anan'ev, M. Y. Boltoeva, L. M. Sharygin, M. S. Grigor'ev and V. P. Shilov, *Radiochemistry*, 2006, **48**, 119–124.
20 M. S. Tyumentsev, A. V. Anan'ev, T. S. Lapitskaya and G. L. Bykov, *Radiochemistry*, 2013, **55**, 279–286.
21 G. Liang, Y. Li, C. Yang, X. Hu, Q. Li and W. Zhao, *RSC Adv.*, 2021, **11**, 22365–22375.
22 Y. Liu, W. Shao, Y. Zheng, C. Zhang, W. Zhou, X. Zhang and Y. Liu, *RSC Adv.*, 2020, **10**, 26451–26459.
23 A. P. Hawkins, A. Zachariou, S. F. Parker, P. Collier, N. Barrow, I. P. Silverwood, R. F. Howe and D. Lennon, *RSC Adv.*, 2020, **10**, 23136–23147.
24 L. Zhu, F. Xiao, Z. Zhang, Y. Sun, Y. Han and S. Qiu, *Catal. Today*, 2001, **68**, 209–216.
25 Z. Li, X. Jiang, G. Xiong, B. Nie, C. Liu, N. He and J. Liu, *Catal. Sci. Technol.*, 2020, **10**, 7829–7841.
26 P. Schneider, *Appl. Catal., A*, 1995, **129**, 157–165.
27 C. He, P. Li, J. Cheng, H. Wang, J. Li, Q. Li and Z. Hao, *Appl. Catal., A*, 2010, **382**, 167–175.
28 C. Christensen, K. Johannsen, E. Tornqvist, I. Schmidt, H. Topsoe and C. Christensen, *Catal. Today*, 2007, **128**, 117–122.
29 X. Guo, X. Wang, J. Guan, X. Chen, Z. Qin, X. Mu and M. Xian, *Chin. J. Catal.*, 2014, **35**, 733–740.
30 C. Hernandez-Mejia, E. S. Gnanakumar, A. Olivos-Suarez, J. Gascon, H. F. Greer, W. Zhou, G. Rothenberg and N. Raveendran Shiju, *Catal. Sci. Technol.*, 2016, **6**, 577–582.
31 C. Dong, H. Wang, H. Du, J. Peng, Y. Cai, S. Guo, J. Zhang, C. Samart and M. Ding, *Mol. Catal.*, 2020, **482**, 110755.
32 A. V. Anan'ev, M. Y. Boltoeva, M. S. Tyumentsev and I. G. Tananaev, *Radiochemistry*, 2013, **55**, 158–161.
33 J. R. Pembridge and G. Stedman, *J. Inorg. Nucl. Chem.*, 1981, **43**, 2859–2862.
34 A. V. Anan'ev and V. P. Shilov, *Radiochemistry*, 2004, **46**, 348–355.
35 J. Fitzpatrick, T. A. Meyer, M. E. O'Neill and D. L. H. Williams, *J. Chem. Soc., Faraday Trans. 2*, 1984, 927–932.